

 Open access • Posted Content • DOI:10.20944/PREPRINTS202006.0249.V1

## **TMPRSS2 Protease Inhibitors May Prolong But Heparins Accelerate SARS-CoV-2 Clearance** — [Source link](#)

Shu Yuan, Si-Cong Jiang, Zhong-Wei Zhang, Zi-Lin Li ...+8 more authors

**Published on:** 21 Jun 2020

**Topics:** Protease

Related papers:

- [Screening strategy of TMPRSS2 inhibitors by FRET-based enzymatic activity for TMPRSS2-based cancer and COVID-19 treatment](#)
- [Structure, activity and inhibition of human TMPRSS2, a protease implicated in SARS-CoV-2 activation](#)
- [Structural analysis of experimental drugs binding to the SARS-CoV-2 target TMPRSS2.](#)
- [Potential protease inhibitors and their combinations to block SARS-CoV-2.](#)
- [A novel class of TMPRSS2 inhibitors potently block SARS-CoV-2 and MERS-CoV viral entry and protect human epithelial lung cells.](#)

Share this paper:    

View more about this paper here: <https://typeset.io/papers/tmpRSS2-protease-inhibitors-may-prolong-but-heparins-2trwvx6rh>

## TM PRSS2 Protease Inhibitors May Prolong But Heparins Accelerate SARS-CoV-2 Clearance

Shu Yuan,<sup>1,5,\*</sup> Si-Cong Jang,<sup>2,5</sup> Zhong-Wei Zhang,<sup>1,5</sup> Zi-Lin Li,<sup>3,5</sup> Chang-Quan Wang,<sup>1</sup> Ming Yuan,<sup>4</sup> Yang-Er Chen,<sup>4</sup> Qi Tao,<sup>1</sup> Ting Lan,<sup>1</sup> Xiao-Yan Tang,<sup>1</sup> Guang-Deng Chen,<sup>1</sup> and Jian Zeng<sup>1</sup>

<sup>1</sup>College of Resources, Sichuan Agricultural University, Chengdu 611130, China

<sup>2</sup>Chengdu KangHong Pharmaceutical Group Comp. Ltd., Chengdu 610036, China

<sup>3</sup>Department of Cardiovascular Surgery, Xijing Hospital, Medical University of the Air Force, Xi'an 710032, China

<sup>4</sup>College of Life Science, Schuan Agricultural University, Ya'an 625014, China

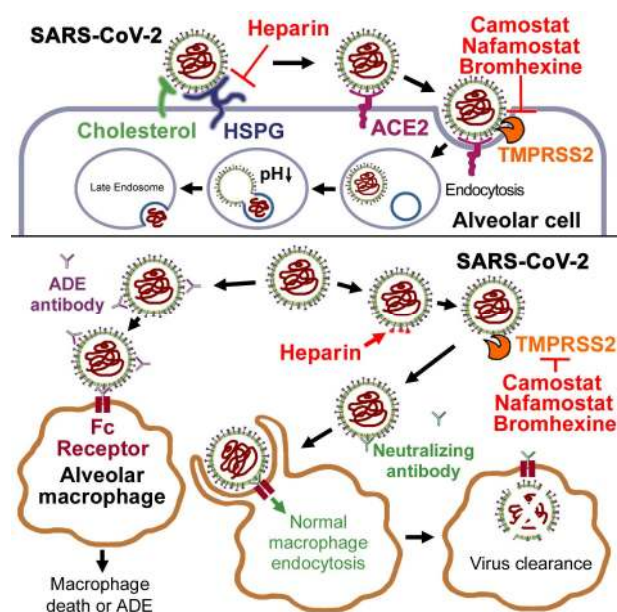
<sup>5</sup>Co-first author

\*Correspondence: [roundtree318@hotmail.com](mailto:roundtree318@hotmail.com) (S.Y.)

### SUMMARY

The 2019 novel SARS-like coronavirus (SARS-CoV-2) entry depends on the host membrane serine protease TM PRSS2, which can be blocked by some clinically-proven drugs. Here we analyzed spatial relevance between glycosylation sequons and antibody epitopes and found that, different from SARS-CoV S, most high-surface-accessible epitopes of SARS-CoV-2 S are blocked by the glycosylation, and the optimal epitope with the highest surface accessibility is covered by the S1 cap. TM PRSS2 inhibitor treatments may prevent unmasking of this epitope and therefore prolong virus clearance and may induce antibody-dependent enhancement. Interestingly, a heparin-binding sequence immediately upstream of the S1/S2 cleavage site has been found in SARS-CoV-2 S but not in SARS-CoV S. Binding of SARS-CoV-2 with heparins may lead to exposure of S686, which then facilitates the S1/S2 cleavage, induces exposure of the optimal epitope, and therefore increases the antibody titres. A combination of heparin and vaccine (or convalescent serum) treatments thus is recommended.

### Graphical Abstract



28  
29  
30

## 1 In Brief

2 Most strong epitopes of SARS-CoV-2 S are blocked by the glycosylation, and the optimal epitope with the  
3 highest surface accessibility is covered by the S1 subunit. Heparin facilitates the S1/S2 cleavage. Therefore,  
4 TMPRSS2 inhibitors may prolong but heparins may accelerate SARS-CoV-2 clearance.

## 6 Highlights

- 7 • Most strong epitopes of SARS-CoV-2 S are covered by glycans or the S1 subunit.
- 8 • TMPRSS2 inhibitor may prevent unmasking of the optimal epitope.
- 9 • Free heparins may induce more exposure of the optimal epitope.
- 10 • Max blood concentrations of TMPRSS2 inhibitors are below  $IC_{90}$ .

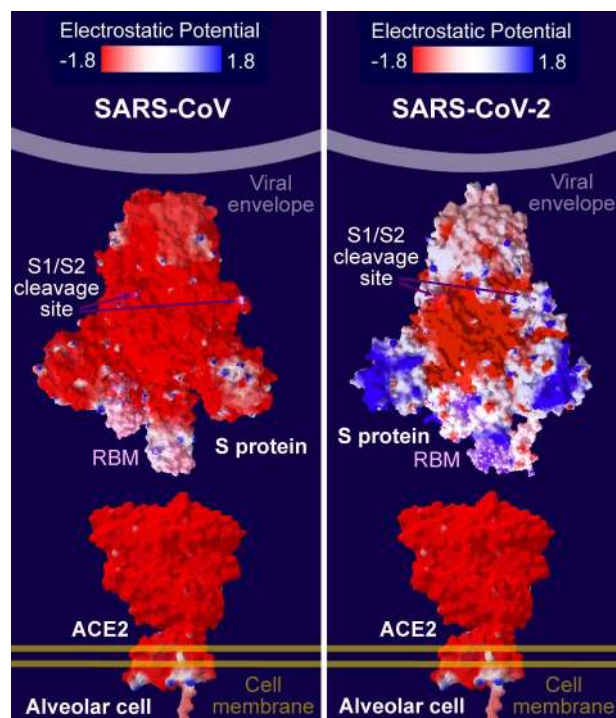
## 12 INTRODUCTION

13 Considering the wide spread of the 2019 novel SARS-like coronavirus (SARS-CoV-2), many candidate drugs  
14 have been proposed and testified. No highly-specific anti-viral treatment exists. Therefore, host-directed  
15 therapies have been repurposed to treat the novel coronavirus disease 2019 (COVID-19), such as some  
16 immunomodulators to prevent the cytokine storm and drugs to inhibit the virus entry or endocytosis  
17 (Zumla et al., 2020).

18 SARS-like coronaviruses utilize angiotensin-converting enzyme 2 (ACE2) as the receptor (Yan et al., 2020).  
19 And a plasma membrane serine protease TMPRSS2 is responsible for the proteolysis of viral spike (S)  
20 proteins in the post-receptor-binding stage (Glowacka et al., 2011; Kawase et al., 2012; Matsuyama et al.,  
21 2010; Shulla et al., 2011; Yamamoto et al., 2016). Viral spike (S) protein S1 attaches the virion to the cell  
22 membrane by interacting with the host receptor, initiating the infection. Binding to human ACE2 receptors  
23 and internalization of the virus into the endosomes of the host cell induce conformational changes in the S  
24 glycoprotein. Proteolysis by TMPRSS2 may unmask the fusion peptide of S2 and activate membranes  
25 fusion within endosomes. Spike protein S2 mediates fusion of the virion and cellular membranes by acting  
26 as a class I viral fusion protein (Xia et al., 2020). Under the current model, the protein has at least three  
27 conformational states: pre-fusion native state, pre-hairpin intermediate state, and post-fusion hairpin state.  
28 During viral and target cell membrane fusion, the coiled coil regions (heptad repeats) assume a trimer-of-  
29 hairpins structure, positioning the fusion peptide in close proximity to the C-terminal region of the  
30 ectodomain. The formation of this structure appears to drive apposition and subsequent fusion of viral  
31 and target cell membranes (Xia et al., 2020).

32 Recently, Hoffmann et al. (2020) found that a TMPRSS2 inhibitor camostat blocked CoV infection in-vitro.  
33 Here we analyzed spatial relevance between glycosylation sequons and antibody epitopes and found that,  
34 different from SARS-CoV S, most high-surface-accessible epitopes of SARS-CoV-2 S are blocked by the  
35 glycosylation, and the optimal epitope with the highest surface accessibility is covered by the S1 cap.  
36 TMPRSS2 inhibitor treatments may prevent unmasking of this epitope and therefore prolong virus  
37 clearance subsequently. A clinical study suggested that higher TMPRSS2 levels in prostate cancer patients  
38 did not increase their illness duration after SARS-CoV-2 infections, but decreased the mortality rate  
39 significantly; inhibition to TMPRSS2 (as androgen-deprivation therapy) may not improve the outcomes  
40 (Montopoli et al., 2020). Interestingly, a heparin-binding sequence immediately upstream of the S1/S2  
41 cleavage site has been found in SARS-CoV-2 S but not in SARS-CoV S, indicating that free heparins may  
42 promote the S1/S2 cleavage, induce exposure of the optimal epitope, and therefore accelerate the virus  
43 clearance. This assumption has been proved by a serological study that adding 10  $\mu$ M heparins into the  
44 sera from COVID-19 patients led to a four-fold increase in antibody titres (Perera et al., 2020).

1

2 **RESULTS AND DISCUSSION**3 **Positive Electrostatic Potential of SARS-CoV-2 S Protein May Explain Its High Affinity to ACE2.**

4

5 **Figure 1. Electrostatic Potential of SARS-CoV S, SARS-CoV-2 S and Human ACE2**

6 The red-to-blue color on the molecular surface indicates the electrostatic potential (red: -1.8; blue: 1.8).

7 The S1/S<sub>2</sub> cleavage sites are marked with the dark purple color. The receptor-binding motifs (RBM) are  
8 marked with the pale lavender color.

9

10 The predominant state of the trimer has one of the three receptor-binding domains (RBDs) rotated up in a  
11 receptor-accessible conformation. Biophysical and structural evidences indicated that ACE2 bound to the  
12 SARS-CoV-2 S ectodomain with about 15 nM affinity, which is 10 to 20-fold higher than ACE2 binding to  
13 SARS-CoV S (Yan et al., 2020). Here we calculated electrostatic potential of SARS-CoV S protein,  
14 SARS-CoV-2 S protein and human ACE2 (Figure 1). Interestingly, both SARS-CoV S and ACE2 protein  
15 surfaces are uniformly negatively-charged, and therefore they repel each other. However, a large part of  
16 SARS-CoV-2 S protein surface is electrically neutral but its receptor-binding motif (RBM) is positive-charged,  
17 and therefore SARS-CoV-2 S and ACE2 attract each other. The S1/S<sub>2</sub> cleavage sites are distributed in the  
18 middle of both SARS-CoV S and SARS-CoV-2 S proteins, implying that TMPRSS2-mediated S1/S<sub>2</sub> cleavage  
19 may not influence ACE2 binding.

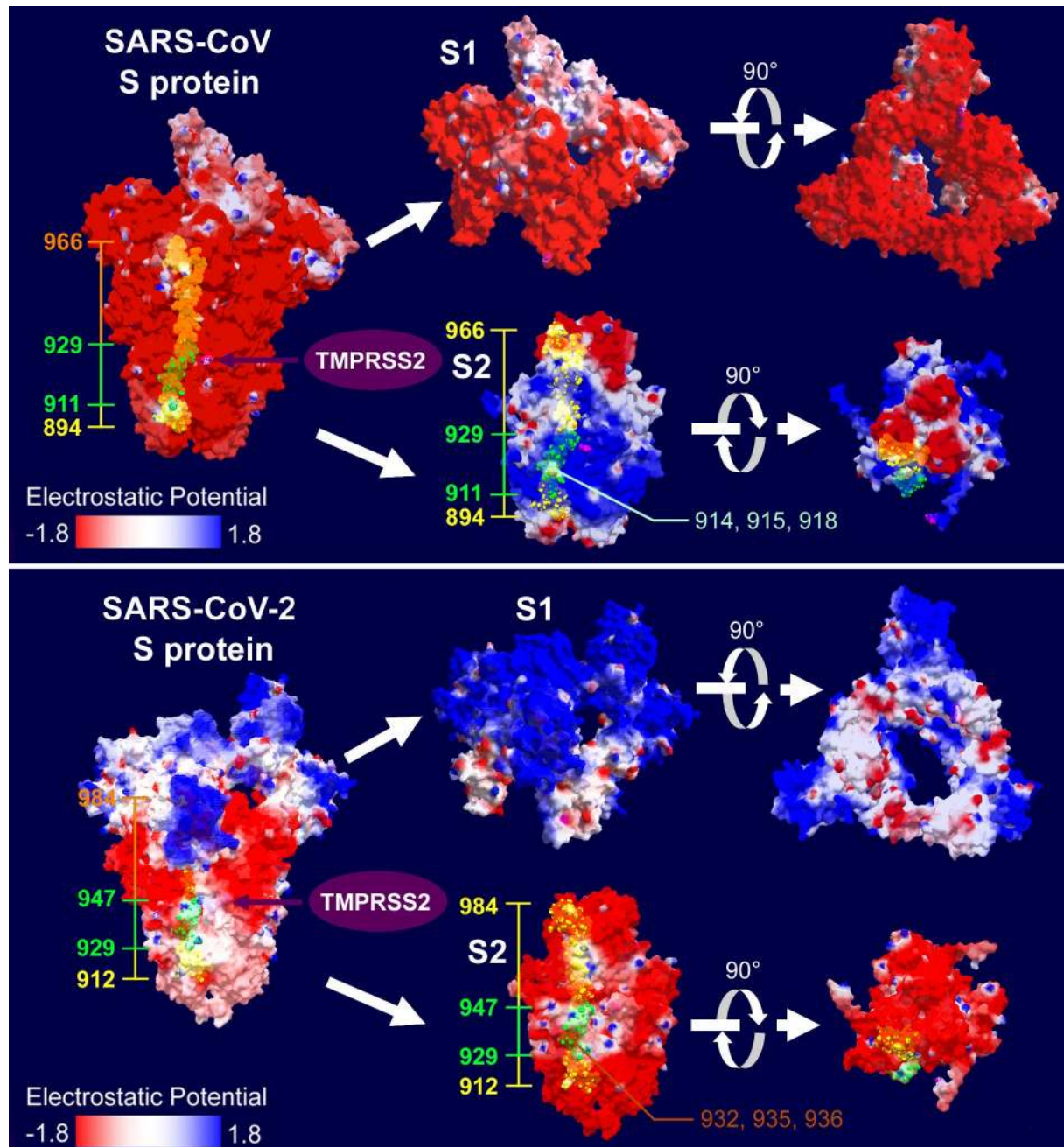
20

21 **SARS-CoV-2 S Fusion Core Peptides Are More Hydrophobic than SARS-CoV S**

22 A study of the X-ray crystal structure revealed that the six-helical fusion core in the SARS-CoV-2 S protein  
23 S<sub>2</sub> subunit is formed by interaction between two heptad repeat domains HR1 and HR2 (Xia et al., 2020).  
24 The three HR1 domains (894-966 of SARS-CoV S protein or 912-984 of SARS-CoV-2 S protein) form a  
25 parallel trimeric coiled-coil center, around which three HR2 domains (1145-1195 of SARS-CoV S protein or  
26 1163-1213 of SARS-CoV-2 S protein) are entwined in an antiparallel manner (Xia et al., 2020). The  
27 interaction between these two domains is predominantly a hydrophobic force. Each pair of two adjacent



1 HR1 helices forms a deep hydrophobic groove, providing the binding site for hydrophobic residues of the  
 2 HR2 domain. The hydrophobic appearance (electrically neutral surface) plays an important role in the  
 3 membrane fusion process (Xia et al., 2020).



4

5 **Figure 2. Electrostatic Potential of SARS-CoV and SARS-CoV-2 S1 and S2 Subunits**

6 The Viral spike (S) protein could be divided into S1 and S2 subunits upon the cleavage by TMPRSS2. The  
 7 red-to-blue color on the molecular surface indicates the electrostatic potential (red: -1.8; blue: 1.8). The  
 8 S1/S2 cleavage sites are marked with the dark purple color. The heptad repeat domain HR1 on one of the  
 9 three monomers is marked with orange (invisible segment covered by the S1 cap), green (the fusion core)  
 10 and yellow colors (visible segment without a cover of S1 cap). In the SARS-CoV fusion core, only three aa  
 11 distribute on an electrically-neutral area (marked with the pale green color); while the others distribute on  
 12 the hydrophilic area. Different from SARS-CoV, the SARS-CoV-2 fusion core is much more hydrophobic that  
 13 only three aa distribute on an electrically-negative area (marked with the brown color) and the others

1 distribute on the electrically-neutral area.

2

3 The SARS-CoV fusion core is composed of 19 amino acids (aa; 911-929 of SARS-CoV S); while the  
4 SARS-CoV-2 fusion core is also composed of 19 aa (929-947 of SARS-CoV-2 S; Figure 2). Interestingly, a  
5 majority of SARS-CoV fusion core peptide surface is negatively-charged, which could be converted into  
6 positive-charged after the TM PRSS2 cleavage, indicating an electrical charge redistribution. Among the 19  
7 aa, only three aa distribute on an electrically-neutral area; while the others distribute on the hydrophilic  
8 area. Different from SARS-CoV, the SARS-CoV-2 fusion core is much more hydrophobic that only three aa  
9 distribute on an electrically-negative area and the others distribute on the electrically-neutral area. More  
10 hydrophobic appearance of SARS-CoV-2 fusion core may be another reason for its higher infectivity  
11 compared to SARS-CoV. Interestingly, C-terminus of HR1 domain in either SARS-CoV S (930-966 aa) or  
12 SARS-CoV-2 S (948-984 aa) is covered by the S1 subunit, which could be unmasked upon proteolysis by  
13 TM PRSS2, also confirming the role of TM PRSS2 in the conformational changes required for the membrane  
14 fusion process.

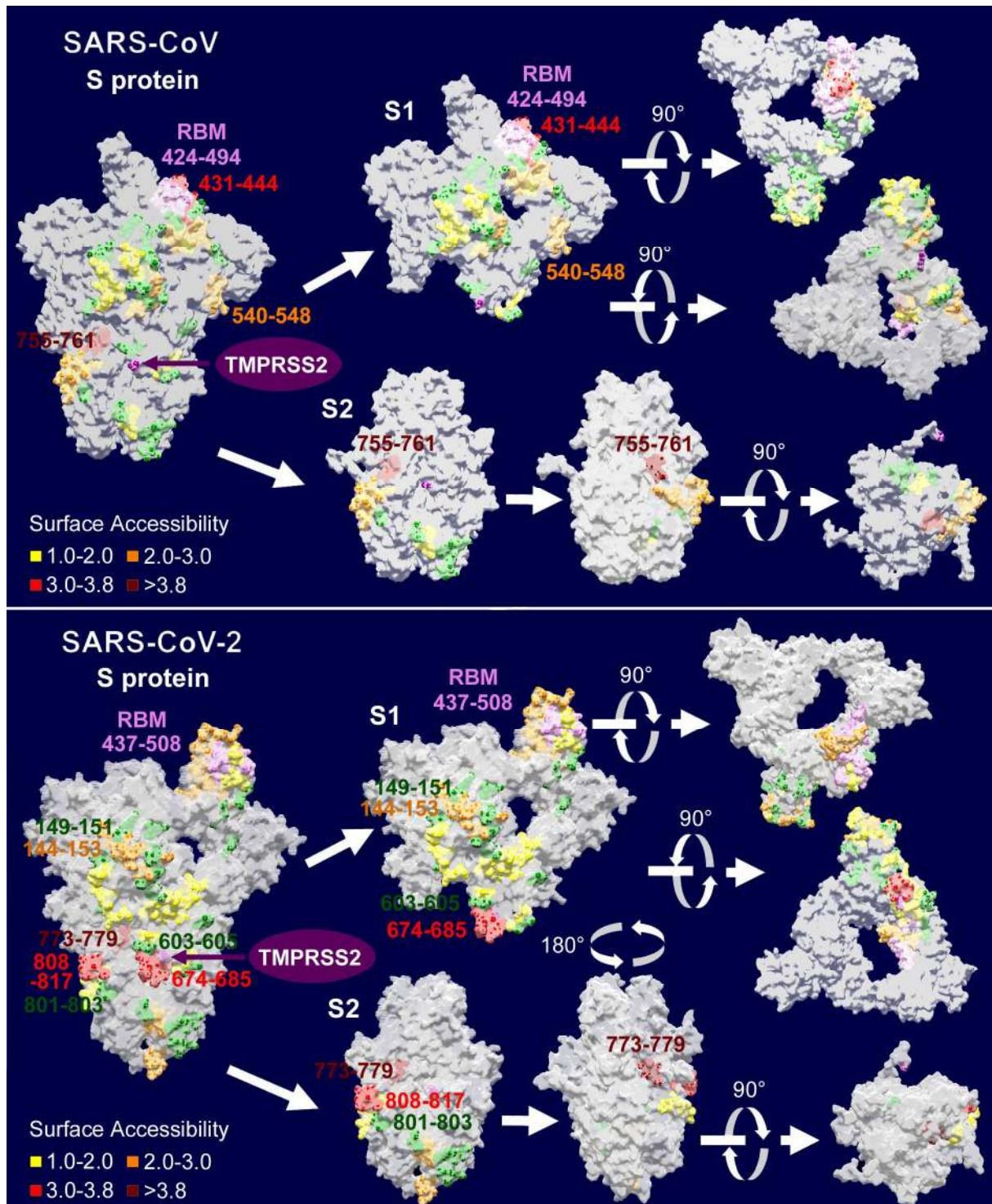
15

### 16 **The Optimal Epitope with the Highest Surface Accessibility Is Covered by the S1 Cap**

17 Being exposed on the viral surface, S proteins are a major target for host antibodies and are referred to as  
18 viral antigens; these antigens are therefore targets for vaccine development (Zheng and Song, 2020).  
19 However, viral envelope proteins are often modified by the attachment of complex glycans. The  
20 glycosylation of these surface antigens helps the pathogen evade recognition by the host immune system  
21 by cloaking the protein surface from detection by antibodies, and can influence the ability of the host to  
22 raise an effective adaptive immune response or even be exploited by the virus to enhance infectivity  
23 (Baum and Cobb, 2017; Pereira et al., 2018).

24 In this study, we computed sequence-based antibody epitopes on spike proteins of SARS-CoV and  
25 SARS-CoV-2 (Tables S1 and S2). As the surface accessibility of epitope is the most important determinant  
26 to the interaction between antibody and antigen, the possible antibody epitopes were filtered with the  
27 surface accessible scores by using the default threshold value of 1.0 (Emini et al., 1985). Then the epitope  
28 candidates were re-scored by using BepiPred-2.0 bioinformatic tool with the default threshold value of  
29 0.50 (Jespersen et al., 2017). 27 epitopes were found on SARS-CoV S protein, among which 10 epitopes  
30 had been ruled out due to the low epitope scores. And 30 epitopes were identified on SARS-CoV-2 S,  
31 among which 9 epitopes had been ruled out due to the low epitope scores (Tables S1 and S2). In SARS-CoV  
32 RBD region (306-527) and SARS-CoV-2 RBD region (319-541) respectively, 4 epitopes and 6 epitopes were  
33 screened out finally. Our epitope prediction has been proved by two clinical studies. In one study, 399  
34 human monoclonal antibodies (mAbs) have been sorted in 10 SARS-CoV-2 patients, but only 35  
35 S-protein-specific mAbs were acquired, among which, 4 mAbs recognize RBD (Chi et al., 2020). Another  
36 study indentified the S230 antibody, which was isolated from memory B cells of a SARS-CoV-infected  
37 individual and potently neutralized a broad spectrum of SARS-CoV isolates of human and animal origins  
38 (Rockx et al., 2008). The S230 epitope is centered around L443 on S protein and Y408, Y442, F460 and  
39 Y475 participate binding to this antibody (Rockx et al., 2008), which matches to a 14 aa epitope candidate  
40 (431-444) screened out in this study with a high surface accessibility (SA) score of 3.149 (Table S1).





1  
2 **Figure 3. Distribution of Glycosylation Sequons and Antibody Epitopes on SARS-CoV S and SARS-CoV-2 S**  
3 The Viral spike (S) protein could be divided into S1 and S2 subunits after the cleavage by TM PRSS2. The  
4 S1/ S2 cleavage sites are marked with the dark purple color. The receptor-binding motifs (RBM) are marked  
5 with the pale lavender color. Putative epitopes with different surface accessibilities (SA) are marked with  
6 yellow (SA 1.0-2.0), orange (SA 2.0-3.0), red (SA 3.0-3.8) and brown (SA >3.8) colors. Glycosylation  
7 sequons are marked with the green color. The putatively-optimal epitope (755-761) of SARS-CoV with the  
8 highest SA score of 4.431 is located on the cutting surface of S<sub>2</sub> subunit, which would be uncovered only  
9 after TM PRSS2 cleavage. And the putatively-optimal epitope (773-779) of SARS-CoV-2 with the highest SA

1 score of 4.868 is also located on the cutting surface of S<sub>2</sub> subunit, whose binding requires removal of the  
2 S<sub>1</sub> cap. Due to the coverage limitation in the Swiss model, glycosylation sequons and epitopes in  
3 1120-1255 aa of SARS-CoV S or in 1147-1273 aa of SARS-CoV-2 S are not shown in the figure. To present  
4 the sites more clearly, only one of the three monomers is labeled.

5  
6 Walls et al. (2020) identified N-linked glycosylation sequons in SARS-CoV S and SARS-CoV-2 S. Along  
7 with these data, spatial relevance between glycosylation sequons and antibody epitopes were further  
8 analyzed (Figure 3). Grant et al. (2020) demonstrated that most SARS-CoV and SARS-CoV-2 epitopes are  
9 shielded by glycans, and only areas of the protein surface at the apex of the S<sub>1</sub> domain appear to be  
10 accessible to known antibodies (Vankadari and Wilce, 2020). A visual examination of the structures from  
11 molecular dynamics simulation also confirmed that the most exposed epitopes comprise the ACE2  
12 receptor site RBD, specifically at the apex region of the RBM domain (Grant et al., 2020). Similar results  
13 were also obtained in this study. On SARS-CoV S, only three strong epitopes with SA scores >3.0 have been  
14 identified. One epitope (431-444; matching to the S<sub>230</sub> epitope as mentioned above) recognizes RBD and  
15 is not surrounded by glycosylation sequons. Another epitope (1238-1243) is located in the C-terminal  
16 transmembrane domain (Figure S1) and therefore should not be accessible to any antibody. The  
17 putatively-optimal epitope (755-761) with the highest SA score of 4.431 is located on the cutting surface of  
18 S<sub>2</sub> subunit, which could be uncovered only after TM PRSS2 cleavage (Figure 3). Besides, the epitope  
19 540-548 is also not surrounded by glycosylation sequons, however its relatively low SA score (2.396) may  
20 suggest a low neutralizing ability (Figure 3 and Figure S2).

21 Unfortunately, no strong epitopes (SA scores >3.0) is available that recognizes SARS-CoV-2 RBD. This  
22 finding is consistent with the fact that only low level of binding of SARS-CoV-2 S to polyclonal rabbit  
23 anti-SARS S<sub>1</sub> antibodies T62 was detected (Ou et al., 2020). Two strong epitopes are located on  
24 SARS-CoV-2 S<sub>1</sub> (674-685) and S<sub>2</sub> (808-817) subunit surfaces respectively. However both of them are  
25 accompanied with glycosylation sequons. Although these two epitopes have large surface areas, their  
26 accompanying glycosylation sequons are located on raised areas, and therefore may form the steric  
27 hindrance (Figure 3). There is also a strong epitope (1256-1261) located in the C-terminal transmembrane  
28 domain (Figure S1). And the putatively-optimal epitope (773-779) with the highest SA score of 4.868 is  
29 also located on the cutting surface of S<sub>2</sub> subunit, whose binding requires removal of the S<sub>1</sub> cap (Figure 3).  
30 Notably, a remarkable alterations in the antigenicity was observed in SARS-CoV-2 that no strong  
31 RBD-targeting epitopes is available and almost all high-surface-accessible epitopes are blocked by the  
32 glycosylation, including the 4A8 epitope sorted recently (matching to a 10 aa epitope 144-153 identified  
33 in this study; Chi et al., 2020). These results might explain why the sera from convalescent SARS-CoV-2  
34 patients exhibited a much weaker neutralizing antibody response compared to SARS-CoV (Hoffmann et al.,  
35 2020).

36 These results also imply that developing of monoclonal antibodies may not be an idea strategy to treat  
37 SARS-CoV-2 infections. Alternatively, recombinant virus vector vaccines, DNA vaccines or inactivated virus  
38 vaccines may induce strong cellular immunity rather than humoral immunity that produces antibodies  
39 (Chandrashekar et al., 2020; Gao et al., 2020; Yu et al., 2020; Zhu et al., 2020).

#### 41 **TM PRSS2 Protease Inhibitors May Prolong SARS-CoV-2 Clearance and Induce Antibody-Dependent** 42 **Enhancement**

43 Considering that almost all high-surface-accessible epitopes of SARS-CoV-2 are blocked by the glycan  
44 shield, people may deduce that the virus should not be cleaned up by the immune system. But that is not



1 the truth. The epitope on the cutting surface usually have no time to bind with the corresponding  
2 antibody, since the membrane fusion occurs immediately following the S1/S2 cleavage. However, free  
3 TMPRSS2 makes the antibody binding possible. TMPRSS2 is a secreted protease that is highly expressed in  
4 prostate and lung tissues, especially in secretory epithelia (Afar et al., 2001; Lukassen et al., 2020).  
5 TMPRSS2 inactive precursor is a 492 residue protein classified as a type II transmembrane protein, with a  
6 70 amino acid N-terminal cytoplasmic domain, followed by a 36 amino acid transmembrane domain  
7 (Lucas et al., 2008). Upon sorting to the cytomembrane, the proenzyme would be converted into the  
8 active enzyme through limited proteolysis and removal of both the N-terminal segment and the  
9 transmembrane domain (Figure S1; Khan and James, 1998; Lucas et al., 2008). Then the active enzymes  
10 (C-terminal) may detach from the membrane and be released (secreted) to the extracellular space. As a  
11 result, a small part of SARS-CoV-2 S proteins may be cleaved by free TMPRSS2 before they bind the  
12 receptor ACE2 and then the epitope on the cutting surface may have a time to induce a neutralizing  
13 antibody response, although maybe in a low efficiency. Clinical data suggested that SARS-CoV-2 can be  
14 cleaned up within 17 days (13–22 days; Xu et al., 2020); while the median duration of SARS-CoV RNA  
15 detection is 13 days (6–23 days; Hui et al., 2004).

16 Some TMPRSS2 inhibitors (such as camostat and nafamostat) block the Middle East respiratory  
17 syndrome coronavirus (MERS-CoV) or SARS-CoV infection in-vitro (Kawase et al., 2012; Yamamoto et al.,  
18 2016). Hoffmann et al. (2020) further indicated that camostat mesylate treatment significantly inhibited  
19 SARS-CoV-2 entry into primary human lung cells. However as analyzed above, the optimal epitope with  
20 the highest surface accessibility is covered by the S1 cap and thus TMPRSS2 inhibitors may prevent  
21 unmasking of this epitope and prolong virus clearance subsequently. Nevertheless, the delay in virus  
22 clearance caused by TMPRSS2 inhibitors may not occur in SARS-CoV infections, because that the  
23 neutralizing antibody S230 would play a crucial role in the virus clearance (Rockx et al., 2008).

24 Antibody-dependent enhancement (ADE) of viral entry has been a major concern for epidemiology,  
25 vaccine development, and antibody-based drug therapy (Wan et al., 2020). The ADE antibody binds to the  
26 surface spike protein of coronaviruses, triggers a conformational change of the spike via receptor  
27 functional mimicry (Walls et al., 2019), and mediates viral entry into IgG Fc receptor-expressing cells (like  
28 macrophages) and causes cell death (Wan et al., 2020). Critically, patients who eventually died of SARS  
29 displayed similarly accumulated pulmonary proinflammatory, absence of wound-healing macrophages,  
30 faster neutralizing antibody responses and higher total antibody titer, all of which indicate a certain level  
31 of ADE (Cao, 2020; Tetro, 2020; Zhang et al., 2020; Zhao et al., 2020).

32 Given that TMPRSS2 inhibitors prevent unmasking of the optimal epitope and thus hamper neutralizing  
33 antibody activities, these inhibitors may prolong the persistence of ADE. Although TMPRSS2 inhibitors may  
34 prevent macrophage death caused by the SARS-CoV-2 entry, they increase the likelihood of viral  
35 attachment to the macrophage surface. Alveolar macrophages underwent functional polarization after  
36 such viral attachment, demonstrating a proinflammatory characteristic (Liu et al., 2019). On the other  
37 hand, viral attachment to the macrophage surface may further enhance the infectivity via macrophage  
38 infiltration, which may worsen the lung injury (Li et al., 2020).

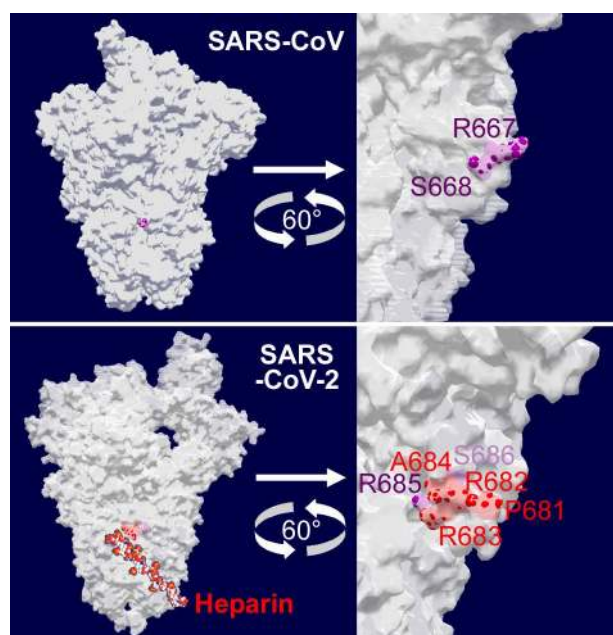
39 These assumptions have been partly proved in prostate cancer patients infected with SARS-CoV-2  
40 (Montopoli et al., 2020). TMPRSS2 is highly expressed in both localized and metastatic prostate cancers  
41 and its transcription is regulated by the androgen receptor. Intriguingly, it has been shown that androgen  
42 positively regulates TMPRSS2 expression also in non-prostatic tissues, including lung (Stopsack et al., 2020).  
43 Montopoli et al. (2020) indicated that 27.2% (31/114) of prostate cancer COVID-19 male patients without  
44 androgen-deprivation therapy developed severe diseases and 15.8% (18/114) died; 28.5% (89/312) of male

1 patients with other tumors and SARS-CoV-2 developed severe diseases and 18.3% (57/312) died; while  
 2 among male patients without cancer 10.0% (411/4102) developed severe diseases and 5.8% (237/4102)  
 3 died. Although only four prostate cancer patients receiving androgen-deprivation therapy were infected  
 4 with SARS-CoV-2, one patient (1/4) still developed severe diseases. These clinical data imply that higher  
 5 TMPRSS2 levels in prostate cancer patients did not increase their illness duration, but decreased the  
 6 mortality rate significantly; inhibition to TMPRSS2 (as androgen-deprivation therapy) may not improve the  
 7 outcomes.

8 Nevertheless, only 4 of 5273 (0.076%) prostate cancer patients receiving androgen-deprivation therapy  
 9 were infected with SARS-CoV-2; while 114 of 37,161 (0.307%) prostate cancer patients without  
 10 androgen-deprivation therapy were infected with SARS-CoV-2. The infection rate decreased by 75.1% after  
 11 the androgen-deprivation therapy. Camostat, nafamostat, or other TMPRSS2 inhibitors (e.g. bromhexine  
 12 as recommended by Stopsack et al., 2020) may be used as prophylactic drugs to reduce the risk of  
 13 infection, because that TMPRSS2 inhibitors may decrease the initial viral load during the incubation period.  
 14 However they may be inefficient for the patients who already develop symptoms, or even have a  
 15 detrimental effect on the virus clearance.

16

#### 17 Heparin May Accelerate SARS-CoV-2 Clearance by Facilitating S1/ S2 Cleavage



18

19 **Figure 4. Distribution of a Heparin-Binding Sequence Immediately Upstream of the S1/ S2 Cleavage Site**  
 20 **on SARS-CoV-2 S But Not on SARS-CoV S**

21 A heparin-binding sequence immediately upstream of the S1/S2 cleavage site has been found in  
 22 SARS-CoV-2 S but not in SARS-CoV S. The heparin-binding sequence is marked with the red color. Both  
 23 R667 and S668 in SARS-CoV S cleavage site are exposed on the protein surface (marked with the dark  
 24 purple color). Contrastingly, although R685 in SARS-CoV-2 S cleavage site is exposed on the protein surface  
 25 (marked with the dark purple color), S686 in SARS-CoV-2 S is embedded under the protein surface (marked  
 26 with the light purple color), which may be exposed above the protein surface via a conformational change  
 27 induced by the heparin binding. To present the sites more clearly, only one of the three monomers is  
 28 labeled.

29

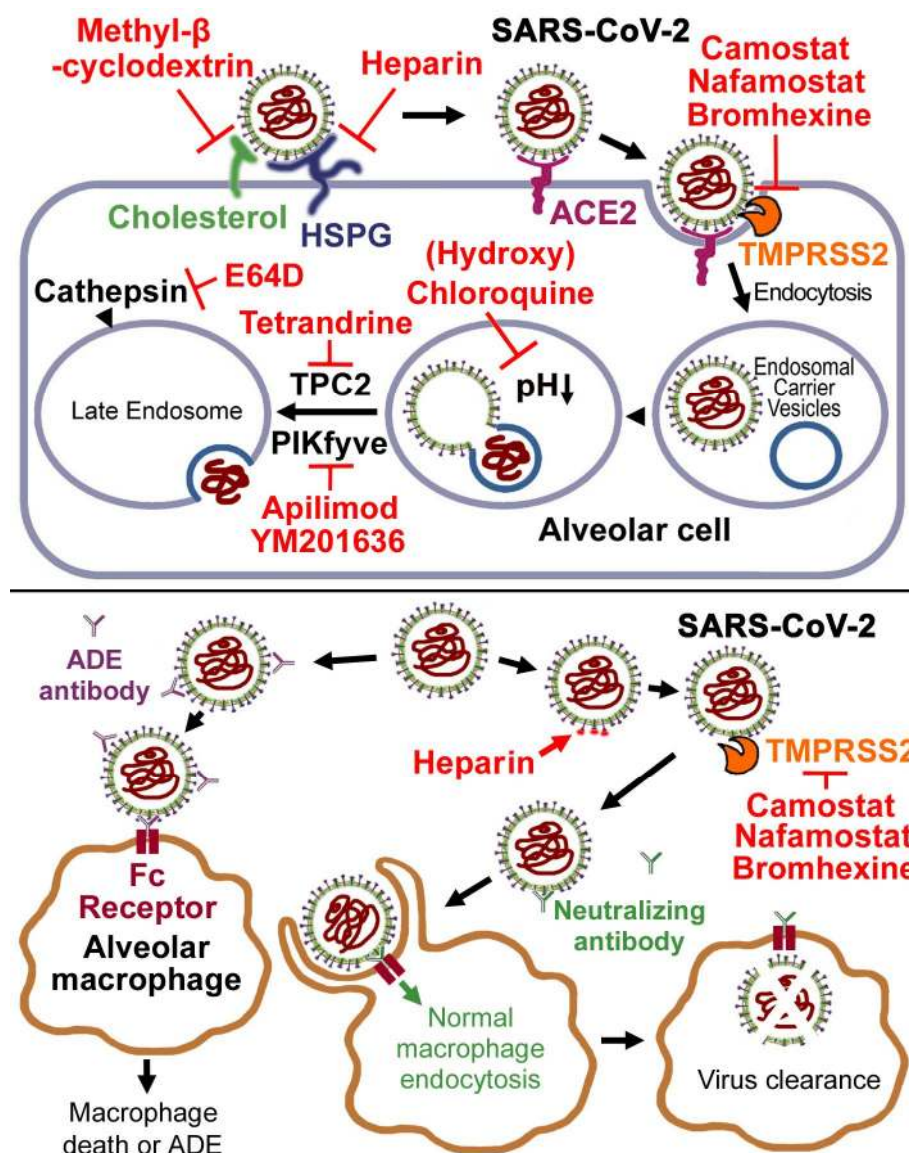
1 Heparin is a mucopolysaccharide sulfuric acid ester that is found especially in the liver and lungs. Heparin  
2 is an attractive target for viral adhesion because of its physiological location on the surface of most animal  
3 cells, where the initial interactions with viruses occur (de Haan et al., 2005). Previous studies found the  
4 heparan sulfate (HS) binding in the S1/S2 cleavage motif of murine coronaviruses (de Haan et al., 2005;  
5 Watanabe et al., 2007). Although heparin is not a direct entry receptor for some murine coronaviruses, it  
6 induces a conformational change of S1 subunit, which may facilitate the virus entry (Mycroft-West et al.,  
7 2020). Here we searched putative HS-binding consensus sequences (XBBXB, XBXB or XBXXBBX; X=any  
8 amino acid, B=basic amino acid; de Haan et al., 2005; Watanabe et al., 2007) on both SARS-CoV S and  
9 SARS-CoV-2 S, and interestingly found that only SARS-CoV-2 S has a HS-binding sequence (681-686 PRRARS)  
10 immediately upstream of the S1/S2 cleavage site (R685-S686; Figure 4). Another intriguing difference  
11 between SARS-CoV S and SARS-CoV-2 S is that both R667 and S668 in SARS-CoV S cleavage site are  
12 exposed on the protein surface, but S686 in SARS-CoV-2 S is embedded under the protein surface (Figure  
13 4). These findings imply that heparin binding may be required for SARS-CoV-2 S1/S2 cleavage, but not for  
14 SARS-CoV S1/S2 cleavage. Binding of SARS-CoV-2 with membrane-bound heparins may lead to exposure of  
15 S686 by a conformational change, which then facilitates the S1/S2 cleavage and the subsequent  
16 membrane fusion (virus entry). While if SARS-CoV-2 S binds free heparins in the interstitial fluids or in the  
17 blood, the enhanced S1/S2 cleavage may induce more exposure of the optimal epitope 773-779, which  
18 therefore accelerates SARS-CoV-2 clearance (Figure 5). One copy of the HS-binding motif adjacent to the  
19 cleavage site in the S protein is a common characteristic of murine coronaviruses (de Haan et al., 2005;  
20 Watanabe et al., 2007), which suggests that one or more rodent species might be the intermediate hosts  
21 of SARS-CoV-2 where the virus was once circulating and mutating (Yuan et al., 2020a).

22 The enhancement to antigenicity by free heparins has been confirmed by a serological assay (Perera et  
23 al., 2020). They observed a 1.0–1.5 log<sub>10</sub> reduction in TCID<sub>50</sub> (median tissue culture infective dose) when  
24 the SARS-CoV-2 was diluted in the heparin medium compared with the control medium. They also carried  
25 out titrations of three sera (from COVID-19 patients) with known micro-neutralisation antibody titres of  
26 1:40, 1:80 and 1:80, with the serum dilutions carried out in parallel in heparin medium or the control  
27 medium without heparin. The antibody titres in the sera diluted in the heparin medium were 1:160, 1:320  
28 and 1:320 respectively (Perera et al., 2020). These results suggested that heparin (heparinised plasma  
29 usually contains about 10 μM heparins) may induce a four-fold increase in the antibody titres against  
30 SARS-CoV-2. A combination of heparin and vaccine (or convalescent serum) treatments may help to  
31 enhance the efficiency of the antibodies.

32 Besides above mechanism, free heparins may also inhibit coronavirus entry by preventing viral adhesion  
33 on the cell surface. SARS-CoV rolls onto the cell membrane by binding to cell-surface cholesterol (Wang et  
34 al., 2008) and heparan sulfate proteoglycans (HSPGs; Lang et al., 2011) and scans for the specific entry  
35 receptor ACE2, which leads to subsequent cell entry (Figure 5). Methyl-β-cyclodextrin (MβCD), an  
36 oligosaccharide used to deplete cholesterol from cell membranes was shown to inhibit SARS-CoV entry in  
37 a dose-dependent manner (although the 90% inhibitory concentration IC<sub>90</sub> was as high as 10 mM; Wang et  
38 al., 2008). Similarly, heparin treatments inhibited SARS-pseudovirus adhesion on the cell surface in a  
39 dose-dependent manner with a IC<sub>90</sub> of about 20 μM (Lang et al., 2011). According to above analysis of  
40 spatial relevance between the heparin-binding sequence and the S1/S2 cleavage site on SARS-CoV-2 S, a  
41 much lower IC<sub>90</sub> specific to SARS-CoV-2 could be expected.

42 The therapeutic effects of heparins on SARS-CoV-2 infections have been confirmed clinically.  
43 Anticoagulant therapy with low molecular weight heparin (LMWH) has been suggested to treat COVID-19,  
44 because that the severe patients have the risk of disseminated intravascular coagulation and venous

1 thromboembolism (Ahmed and Anirvan, 2020; Lin et al., 2020; Tang et al., 2020; Yin et al., 2020).  
 2 Moreover, heparin also showed a good therapeutic effect to acute respiratory distress syndrome (ARDS),  
 3 which is a common complication of viral pneumonia (Thompson et al., 2017). Here we added an important  
 4 information that heparin may also inhibit SARS-CoV-2 entry by both enhancing neutralizing antibody titres  
 5 and preventing viral adhesion on the cell surface. Thus, LMWH anticoagulant therapy may also work for  
 6 the non-severe patients. On the other hand, COVID-19 has a prominent feature, that is, a large amount of  
 7 mucus (oedema and plasma exudation) could be found in the small airway, and it may eventually block the  
 8 airway, which may be an important reason for the high mortality after later mechanical ventilation and  
 9 high-flow oxygen inhalation (Barton et al., 2020). Therefore, nebulized heparin, oxygen supply or other  
 10 inhalation therapies should be given at the early stages of COVID-19 (Yuan et al., 2020b).



11  
 12 **Figure 5. Drugs against SARS-CoV-2 Entry and Their Effects on the Virus Clearance**

13 Coronavirus rolls onto the cell membrane by binding to cell-surface cholesterol and heparan sulfate  
 14 proteoglycans (HSPGs) and scans for the specific entry receptor ACE2, which leads to subsequent cell entry.  
 15 Camostat, nafamostat or bromhexine inhibits the plasma membrane protease TMPRSS2, which is  
 16 responsible for the proteolysis of viral S proteins in the post-receptor-binding stage. Methyl-β-cyclodextrin  
 17 and heparin inhibit virus binding with cholesterol and HSPGs respectively. Chloroquine neutralizes acidic



1 pH in the endosome, which is necessary for viral nucleocapsid release into the cytoplasm. PIKfyve  
2 inhibitors apilimod and YM201636, TPC2 inhibitor tetrandrine and cathepsin L inhibitors E64D and SID  
3 26681509 prevent the virus entry. On the other hand, in the interstitial fluids or in the blood, free heparin  
4 binding may lead to exposure of the S1/S2 cleavage site by a conformational change. Then the enhanced  
5 S1/S2 cleavage by free TMPRSS2 may induce more exposure of the optimal epitope 773-779, which  
6 therefore accelerates neutralizing-antibody-mediated SARS-CoV-2 clearance. Contrastingly, TMPRSS2  
7 inhibitors prevent unmasking of the optimal epitope and thus hamper neutralizing antibody activities,  
8 prolonging the virus clearance. Although TMPRSS2 inhibitors may prevent macrophage death caused by  
9 the SARS-CoV-2 entry, they increase the likelihood of viral attachment to the macrophage surface, which  
10 induces proinflammatory responses and antibody-dependent enhancement (ADE).

11

### 12 **All FDA-Approved TMPRSS2 Inhibitors Would Not Achieve the Effective Concentrations, But Nebulized** 13 **Heparin Would Achieve a Local High Concentration**

14  $IC_{50}$  and  $IC_{90}$  of camostat against either SARS-CoV or SARS-CoV-2 were about 1  $\mu$ M and 5  $\mu$ M respectively  
15 (Hoffmann et al., 2020). Although no direct study about nafamostat against SARS-CoV or SARS-CoV-2 is  
16 available, two previous studies showed that  $IC_{50}$  of nafamostat was about 10 times lower than that of  
17 camostat against MERS-CoV (Shirato et al., 2013; Yamamoto et al., 2016). Thus, it can be deduced that  $IC_{50}$   
18 and  $IC_{90}$  of nafamostat against either SARS-CoV or SARS-CoV-2 may be 0.1  $\mu$ M and 0.5  $\mu$ M respectively.  
19 However the maximum blood concentration of camostat at the normal oral dose of 100 mg would achieve  
20 only 0.21  $\mu$ M (Midgley et al., 1994); while the maximum blood concentration of nafamostat injection at  
21 the maximum dose of 40 mg would achieve only 0.27  $\mu$ M (Iwama et al., 1998). Similarly, the maximum  
22 blood concentration of bromhexine at the maximum dose (single oral dose of 32 mg) would achieve only  
23 0.36  $\mu$ M (Bechgaard and Nielsen, 1982); while  $IC_{90}$  of bromhexine on TMPRSS2 activity is about 1  $\mu$ M  
24 (Lucas et al., 2014). In summary, all FDA-approved TMPRSS2 inhibitors would not achieve the effective  
25 blood concentrations. Thus they may neither inhibit SARS-CoV-2 entry, nor reduce the risk of infection  
26 efficiently. More effective TMPRSS2 inhibitors still need to be developed.

27 Contrastingly, nebulized heparin is inhaled directly into the lung, so it can reach a local high  
28 concentration in alveolar cells. Although the alveolar concentration cannot be easily estimated (1 mg/mL  
29 LMWH is usually used for the ultrasonic atomization, which is equal to about 67  $\mu$ M), it may be higher  
30 than 10  $\mu$ M that can induce a 1.0–1.5  $\log_{10}$  reduction in  $TCID_{50}$  of SARS-CoV-2 (Perera et al., 2020).  
31 Nevertheless, given that heparin may cause thrombocytopenia and thrombosis, more clinical trials are still  
32 required to determine the optimal dosage and therapeutic time.

33 Besides TMPRSS2 inhibitors and heparins, other drugs that inhibit coronavirus entry are summarized  
34 and listed in Table 1 and Figure 5. The cellular alkalizers also repress virus entry through neutralizing acidic  
35 pH in the early endosomes, which is necessary for viral nucleocapsid release into the cytoplasm.  
36 Chloroquine and its derivative hydroxychloroquine are such alkalizers and are used clinically as  
37 antimalarial medicines. In-vitro experiments confirmed that chloroquine is highly effective in the control of  
38 SARS-CoV-2 infection (the inhibition ratio of 10  $\mu$ M chloroquine could reach over 90%; Liu et al., 2020;  
39 Wang et al., 2020; Yao et al., 2020). And a recent clinical trial showed that hydroxychloroquine treatment  
40 is significantly associated with viral load reduction and remission of symptoms in COVID-19 patients  
41 (Gautret et al., 2020). However chloroquine did not reduce the duration of Dengue virus type 2 infection  
42 in a human clinical trial and showed several adverse effects, primarily vomiting (Tricou et al., 2010). And  
43 the high-dosage chloroquine may not reduce the mortality rate but cause more instance of QTc interval  
44 greater than 500 milliseconds, showing a cardiac toxicity (Borba et al., 2020). More rigorous clinical trials

1 on SARS-CoV-2 are still required.

2

3 **Table 1. Drugs against SARS-CoV-2 Entry, Their IC<sub>90</sub> and the Demerits**

| Drug's name           | Mechanisms                     | IC <sub>90</sub> to SARS-CoV | IC <sub>90</sub> to SARS-CoV-2 | Demerits   |
|-----------------------|--------------------------------|------------------------------|--------------------------------|--|
| Camostat              | TM PRSS2 inhibitor             | 5 μM                         | 5 μM                           | Max plasma concentration < 0.27 μM and may causing a prolonged virus clearance |
| Nafamostat            |                                | 0.5 μM <sup>*</sup>          | 0.5 μM <sup>*</sup>            |  |
| Bromhexine            |                                | 1 μM to TM PRSS2             |                                |  |
| Methyl-β-cyclodextrin | Cholesterol depletion          | 10 mM                        | N.A.                           | Non-FDA-approved drug with a very high IC <sub>90</sub>                        |
| Heparin               | Cell surface binding inhibitor | 20 μM                        | < 10 μM <sup>†</sup>           | Thrombocytopenia and thrombosis  |
| Chloroquine           | Alkalizer in the endosome      | N.A.                         | 100 μM                         | non-decreased mortality rate with side effects                                 |
| Hydroxy-chloroquine   |                                | N.A.                         | 10 μM                          |  |
| Apilimod              | PIKfyve inhibitor              | 100 nM                       | 100 nM                         | Non-FDA-approved drug with side effects  |
| YM201636              |                                | N.A.                         | 10 μM                          | Non-FDA-approved drug with side effects  |
| Tetrandrine           | TPC2 inhibitor                 | N.A.                         | 3 μg/ml                        | Non-FDA-approved drug with side effects  |
| E64D                  | Cathepsin L inhibitor          | N.A.                         | 2 μM                           | Non-FDA-approved drug with side effects  |
| SID 26681509          |                                | N.A.                         | 30 μM                          | Non-FDA-approved drug with side effects  |

4 <sup>\*</sup> Although no direct study about nafamostat on SARS-CoV or SARS-CoV-2 is available, two previous studies  
5 showed that IC<sub>50</sub> of nafamostat was about 10 times lower than that of camostat against MERS-CoV. Thus, it  
6 could be deduced that IC<sub>90</sub> of nafamostat against either SARS-CoV or SARS-CoV-2 may be 0.5 μM. <sup>†</sup>10 μM  
7 heparins induced a 1.0–1.5 log<sub>10</sub> reduction in TCID<sub>50</sub> of SARS-CoV-2. Thus, it could be deduced that IC<sub>90</sub> of  
8 heparin against SARS-CoV-2 may be < 10 μM. N.A., Not Available.

9

10 SARS-like coronavirus entry was mediated by a clathrin- and caveolae-independent mechanism (Wang  
11 et al., 2008). Drugs against clathrin-mediated endocytosis (e.g. chlorpromazine) or caveolae-dependent  
12 endocytosis (e.g. filipin and nystatin) had no inhibitory effects on the virus entry (Wang et al., 2008). The  
13 clathrin-pathway inhibitor baricitinib (Richardson et al., 2020; Stebbing et al., 2020) may not work as well.  
14 Nevertheless, a recent study demonstrated that phosphatidylinositol 3-phosphate 5-kinase (PIKfyve), two  
15 pore channel subtype 2 (TPC2), and cathepsin L are critical for SARS-CoV-2 entry (Ou et al., 2020), and  
16 PIKfyve inhibitors apilimod and YM201636, TPC2 inhibitor tetrandrine and cathepsin L inhibitors E64D and  
17 SID 26681509 prevent the virus entry (Table 1; Ou et al., 2020). However, none of them are FDA-approved  
18 drug and may have many side effects. In a nutshell, among all FDA-approved drugs against SARS-CoV-2  
19 entry putatively, camostat, nafamostat or bromhexine may be candidate prophylactic drugs, nebulized  
20 heparin may be a promising therapeutic drug, and validity and safety of (hydroxy)chloroquine require  
21 further clinical investigations.

22

## 1 STAR+M METHODS

2 Detailed methods are provided in the online version of this paper and include the following:

### 3 ● KEY RESOURCES TABLE

### 4 ● LEAD CONTACT AND MATERIALS AVAILABILITY

### 5 ● METHOD DETAILS

6 ○ Homology modeling of ACE2 and viral spike proteins

7 ○ Analysis of antibody epitopes

8 ○ Prediction of transmembrane domain

9 ○ Alignment of SARS-CoV and SARS-CoV-2 spike proteins

### 10 ● QUANTIFICATION AND STATISTICAL ANALYSIS

### 11 ● DATA AND CODE AVAILABILITY

12

## 13 ACKNOWLEDGMENTS

14 This work was supported by the Supporting Program of Sichuan Agricultural University to S.Y.

15

## 16 AUTHOR CONTRIBUTIONS

17 Conceptualization, S.Y.; Formal analysis, S.Y., S.C.J., Z.W.Z. and Z.L.L.; Investigation, C.Q.W., M.Y., Y.E.C., Q.T.,  
18 T.L., X.Y.T., G.D.C and Z.J.; Writing – Original Draft, S.Y.; Writing – Review & Editing, all authors; Funding  
19 acquisition, S.Y.

20

## 21 DECLARATION OF INTERESTS

22 The authors declare no competing interests.

23

## 24 REFERENCES

25 Afar, D. E., Vivanco, I., Hubert, R. S., Kuo, J., Chen, E., Saffran, D. C., Raitano, A. B., and Jakobovits, A. (2001).  
26 Catalytic cleavage of the androgen-regulated TMPRSS2 protease results in its secretion by prostate and  
27 prostate cancer epithelia. *Cancer Res.* 61, 1686–1692.

28 Ahmed, S., and Anirvan, P. (2020). Reply to Rheumatologists' perspective on coronavirus disease 19: is  
29 heparin the dark horse for COVID-19?. *Clin. Rheumatol.* DOI: 10.1007/s10067-020-05145-w.

30 Barton, L. M., Duval, E. J., Stroberg, E., Ghosh, S., and Mukhopadhyay, S. (2020). COVID-19 Autopsies,  
31 Oklahoma, USA. *Am. J. Clin. Pathol.* 153, 725–733.

32 Baum, L. G., and Cobb, B. A. (2017). The direct and indirect effects of glycans on immune function.  
33 *Glycobiology* 27, 619–624.

34 Bechgaard, E., and Nielsen, A. (1982). Bioavailability of bromhexine tablets and preliminary  
35 pharmacokinetics in humans. *Biopharm. Drug Dispos.* 3, 337–344.

36 Bertoni, M., Kiefer, F., Biasini, M., Bordoli, L., and Schwede, T. (2017). Modeling protein quaternary  
37 structure of homo- and hetero-oligomers beyond binary interactions by homology. *Sci. Rep.* 7, 10480.

38 Biasini, M., Bienert, S., Waterhouse, A., Arnold, K., Studer, G., Schmidt, T., Kiefer, F., Gallo Cassarino, T.,  
39 Bertoni, M., Bordoli, L., et al. (2014). SWISS-MODEL: modelling protein tertiary and quaternary structure  
40 using evolutionary information. *Nucleic Acids Res.* 42, W252–W258.

41 Bienert, S., Waterhouse, A., de Beer, T. A. P., Tauriello, G., Studer, G., Bordoli, L., and Schwede, T. (2017).  
42 The SWISS-MODEL Repository - new features and functionality. *Nucleic Acids Res.* 45, D313–D319.

43 Borba, M. G. S., Val, F., Sampaio, V. S., Alexandre, M., Melo, G. C., Brito, M., Mourão, M., Brito-Sousa, J. D.,  
44 Baía-da-Silva, D., Guerra, M., et al. (2020). Effect of high vs low doses of chloroquine diphosphate as

- 1 adjunctive therapy for patients hospitalized with severe acute respiratory syndrome coronavirus 2  
2 (SARS-CoV-2) infection: a randomized clinical trial. *JAMA Network Open* 3, e208857.
- 3 Cao, X. (2020). COVID-19: immunopathology and its implications for therapy[J]. *Nat. Rev. Immunol.* 20,  
4 269–270.
- 5 Chandrashekar, A., Liu, J., Martinot, A. J., McMahan, K., Mercado, N. B., Peter, L., Tostanoski, L. H., Yu, J.,  
6 Maliga, Z., Nekorchuk, M., et al. (2020). SARS-CoV-2 infection protects against rechallenge in rhesus  
7 macaques. *Science* DOI: 10.1126/science.abc4776.
- 8 Chi, X., Yan, R., Zhang, J., Zhang, G., Zhang, Y., Hao, M., Zhang, Z., Fan, P., Dong, Y., Yang, Y., et al. (2020). A  
9 potent neutralizing human antibody reveals the N-terminal domain of the Spike protein of SARS-CoV-2 as a  
10 site of vulnerability. *bioRxiv* DOI: 10.1101/2020.05.08.083964.
- 11 de Haan, C. A., Li, Z., te Lintelo, E., Bosch, B. J., Haijema, B. J., and Rottier, P. J. (2005). Murine coronavirus  
12 with an extended host range uses heparan sulfate as an entry receptor. *J. Virol.* 79, 14451–14456.
- 13 Emini, E. A., Hughes, J. V., Perlow, D. S., and Boger, J. (1985). Induction of hepatitis A virus neutralizing  
14 antibody by a virus-specific synthetic peptide. *J. Virol.* 55, 836–839.
- 15 Forster, P., Forster, L., Penfrew, C., and Forster, M. (2020). Phylogenetic network analysis of SARS-CoV-2  
16 genomes. *Proc. Natl. Acad. Sci. USA* 117, 9241–9243.
- 17 Gao, Q., Bao, L., Mao, H., Wang, L., Xu, K., Yang, M., Li, Y., Zhu, L., Wang, N., Lv, Z., et al. Development of an  
18 inactivated vaccine candidate for SARS-CoV-2. *Science* DOI: 10.1126/science.abc1932.
- 19 Gautret, P., Lagier, J. C., Parola, P., Hoang, V. T., Meddeb, L., Mailhe, M., Doudier, B., Courjon, J.,  
20 Giordanengo, V., Vieira, V. E., et al. (2020). Hydroxychloroquine and azithromycin as a treatment of  
21 COVID-19: results of an open-label non-randomized clinical trial. *Int. J. Antimicrob. Agents* DOI:  
22 10.1016/j.ijantimicag.2020.105949.
- 23 Glowacka, I., Bertram, S., Müller, M. A., Allen, P., Soilleux, E., Pfefferle, S., Steffen, I., Tsegaye, T. S., He, Y.,  
24 Gnirss, K., et al. (2011). Evidence that TMPRSS2 activates the severe acute respiratory syndrome  
25 coronavirus spike protein for membrane fusion and reduces viral control by the humoral immune response.  
26 *J. Virol.* 85, 4122–4134.
- 27 Grant, O. C., Montgomery, D., Ito, K., and Woods, R. J. (2020). 3D Models of glycosylated SARS-CoV-2 spike  
28 protein suggest challenges and opportunities for vaccine development. *bioRxiv* DOI:  
29 10.1101/2020.04.07.030445.
- 30 Hoffmann, M., Kleine-Weber, H., Schroeder, S., Krüger, N., Herrler, T., Erichsen, S., Schiergens, T. S., Herrler,  
31 G., Wu, N. H., Nitsche, A., et al. (2020). SARS-CoV-2 cell entry depends on ACE2 and TMPRSS2 and is  
32 blocked by a clinically proven protease inhibitor. *Cell* 181, 271–280.
- 33 Hui, D. S., Chan, M. C., Wu, A. K., and Ng, P. C. (2004). Severe acute respiratory syndrome (SARS):  
34 epidemiology and clinical features. *Postgrad. Med. J.* 80, 373–381.
- 35 Iwama, H., Nakane, M., Ohmori, S., Kaneko, T., Kato, M., Watanabe, K., and Okuaki, A. (1998). Nafamostat  
36 mesilate, a kallikrein inhibitor, prevents pain on injection with propofol. *Br. J. Anaesth.* 81, 963–964.
- 37 Jespersen, M. C., Peters, B., Nielsen, M., and Marcatili, P. (2017). BepiPred-2.0: improving sequence-based  
38 B-cell epitope prediction using conformational epitopes. *Nucleic Acids Res.* 45, W24–W29.
- 39 Kawase, M., Shirato, K., van der Hoek, L., Taguchi, F., and Matsuyama, S. (2012). Simultaneous treatment  
40 of human bronchial epithelial cells with serine and cysteine protease inhibitors prevents severe acute  
41 respiratory syndrome coronavirus entry. *J. Virol.* 86, 6537–6545.
- 42 Khan, A. R., and James, M. N. (1998). Molecular mechanisms for the conversion of zymogens to active  
43 proteolytic enzymes. *Protein Sci.* 7, 815–836.
- 44 Krogh, A., Larsson, B., von Heijne, G., and Sonnhammer, E. L. L. (2001). Predicting transmembrane protein



- 1 topology with a hidden Markov model: Application to complete genomes. *J. Mol. Biol.* 305, 567–580.
- 2 Lang, J., Yang, N., Deng, J., Liu, K., Yang, P., Zhang, G., and Jiang, C. (2011). Inhibition of SARS pseudovirus  
3 cell entry by lactoferrin binding to heparan sulfate proteoglycans. *PLoS One* 6, e23710.
- 4 Larkin, M. A., Blackshields, G., Brown, N. P., Chenna, R., McGettigan, P. A., McWilliam, H., Valentin, F.,  
5 Wallace, I. M., Wilm, A., Lopez, R., et al. (2007). Clustal W and Clustal X version 2.0. *Bioinformatics* 23,  
6 2947–2948.
- 7 Li, H., Liu, L., Zhang, D., Xu, J., Dai, H., Tang, N., Su, X., and Cao, B. (2020). SARS-CoV-2 and viral sepsis:  
8 observations and hypotheses. *Lancet* 395, 9–15.
- 9 Lin, L., Lu, L., Cao, W., and Li, T. (2020). Hypothesis for potential pathogenesis of SARS-CoV-2 infection—a  
10 review of immune changes in patients with viral pneumonia. *Emerg. Microbes Infect.* 9, 727–732.
- 11 Liu, L., Wei, Q., Lin, Q., Fang, J., Wang, H., Kwok, H., Tang, H., Nishiura, K., Peng, J., Tan, Z., et al. (2019).  
12 Anti-spike IgG causes severe acute lung injury by skewing macrophage responses during acute SARS-CoV  
13 infection. *JCI insight* 4, e123158.
- 14 Liu, J., Cao, R., Xu, M., Wang, X., Zhang, H., Hu, H., Li, Y., Hu, Z., Zhong, W., and Wang, M. (2020).  
15 Hydroxychloroquine, a less toxic derivative of chloroquine, is effective in inhibiting SARS-CoV-2 infection in  
16 vitro. *Cell Discov.* 6, 16.
- 17 Lucas, J. M., True, L., Hawley, S., Matsumura, M., Morrissey, C., Vessella, R., and Nelson, P. S. (2008). The  
18 androgen-regulated type II serine protease TMPRSS2 is differentially expressed and mislocalized in  
19 prostate adenocarcinoma. *J. Pathol.* 215, 118–125.
- 20 Lucas, J. M., Heinlein, C., Kim, T., Hernandez, S. A., Malik, M. S., True, L. D., Morrissey, C., Corey, E.,  
21 Montgomery, B., Mostaghel, E., et al. (2014). The androgen-regulated protease TMPRSS2 activates a  
22 proteolytic cascade involving components of the tumor microenvironment and promotes prostate cancer  
23 metastasis. *Cancer Discov.* 4, 1310–1325.
- 24 Lukassen, S., Chua, R. L., Trefzer, T., Kahn, N. C., Schneider, M. A., Muley, T., Winter, H., Meister, M., Veith,  
25 C., Boots, A. W., et al. (2020). SARS-CoV-2 receptor ACE2 and TMPRSS2 are primarily expressed in  
26 bronchial transient secretory cells. *EMBO J.* 39, e105114.
- 27 Matsuyama, S., Nagata, N., Shirato, K., Kawase, M., Takeda, M., and Taguchi, F. (2010). Efficient activation  
28 of the severe acute respiratory syndrome coronavirus spike protein by the transmembrane protease  
29 TMPRSS2. *J. Virol.* 84, 12658–12664.
- 30 Midgley, I., Hood, A. J., Proctor, P., Chasseaud, L. F., Irons, S. R., Cheng, K. N., Brindley, C. J., and Bonn, R.  
31 (1994). Metabolic fate of <sup>14</sup>C-camostat mesylate in man, rat and dog after intravenous administration.  
32 *Xenobiotica* 24, 79–92.
- 33 Moller, S., Croning, M. D. R., and Apweiler, R. (2001). Evaluation of methods for the prediction of  
34 membrane spanning regions. *Bioinformatics* 17, 646–653.
- 35 Montopoli, M., Zumerle, S., Vettor, R., Rugge, M., Zorzi, M., Catapano, C. V., Carbone, G. M., Cavalli, A.,  
36 Pagano, F., Ragazzi, E., et al. (2020). Androgen-deprivation therapies for prostate cancer and risk of  
37 infection by SARS-CoV-2: a population-based study (n=4532). *Ann. Oncol.* DOI:  
38 10.1016/j.annonc.2020.04.479.
- 39 Mycroft-West, C., Su, D., Elli, S., Li, Y., Guimond, S., Miller, G., Turnbull, J., Yates, E., Guerrini, M., Fernig, D.,  
40 et al. (2020). The 2019 coronavirus (SARS-CoV-2) surface protein (Spike) S1 Receptor Binding Domain  
41 undergoes conformational change upon heparin binding. *bioRxiv* DOI: 10.1101/2020.02.29.971093.
- 42 Ou, X., Liu, Y., Lei, X., Li, P., Mi, D., Ren, L., Guo, L., Guo, R., Chen, T., Hu, J., et al. (2020). Characterization of  
43 spike glycoprotein of SARS-CoV-2 on virus entry and its immune cross-reactivity with SARS-CoV. *Nat.*  
44 *Commun.* 11, 1620.

- 1 Pereira, M. S., Alves, I., Vicente, M., Campar, A., Silva, M. C., Padrão, N. A., Pinto, V., Fernandes, Â., Dias, A.  
2 M., and Pinho, S. S. (2018). Glycans as key checkpoints of T cell activity and function. *Front. Immunol.* *9*,  
3 2754.
- 4 Perera, R. A., Mok, C. K., Tsang, O. T., Lv, H., Ko, R. L., Wu, N. C., Yuan, M., Leung, W. S., Chan, J. M., Chik, T.  
5 S., et al. (2020). Serological assays for severe acute respiratory syndrome coronavirus 2 (SARS-CoV-2),  
6 March 2020. *Euro Surveill.* *25*, 2000421.
- 7 Richardson, P., Griffin, I., Tucker, C., Smith, D., Oechsle, O., Phelan, A., and Stebbing, J. (2020). Baricitinib as  
8 potential treatment for 2019-nCoV acute respiratory disease. *Lancet* *395*, e30–e31.
- 9 Rockx, B., Corti, D., Donaldson, E., Sheahan, T., Stadler, K., Lanzavecchia, A., and Baric, R. (2008). Structural  
10 basis for potent cross-neutralizing human monoclonal antibody protection against lethal human and  
11 zoonotic severe acute respiratory syndrome coronavirus challenge. *J. Virol.* *82*, 3220–3235.
- 12 Shirato, K., Kawase, M., and Matsuyama, S. (2013). Middle East respiratory syndrome coronavirus infection  
13 mediated by the transmembrane serine protease TM<sub>PRSS2</sub>. *J. Virol.* *87*, 12552–12561.
- 14 Shulla, A., Heald-Sargent, T., Subramanya, G., Zhao, J., Perlman, S., and Gallagher, T. (2011). A  
15 transmembrane serine protease is linked to the severe acute respiratory syndrome coronavirus receptor  
16 and activates virus entry. *J. Virol.* *85*, 873–882.
- 17 Stebbing, J., Phelan, A., Griffin, I., Tucker, C., Oechsle, O., Smith, D., and Richardson, P. (2020). COVID-19:  
18 combining antiviral and anti-inflammatory treatments. *Lancet Infect. Dis.* *20*, 400–402.
- 19 Stopsack, K. H., Mucci, L. A., Antonarakis, E. S., Nelson, P. S., and Kantoff, P. W. (2020). *TM<sub>PRSS2</sub>* and  
20 COVID-19: serendipity or opportunity for intervention? *Cancer Discov.* DOI:  
21 10.1158/2159-8290.CD-20-0451.
- 22 Tang, N., Bai, H., Chen, X., Gong, J., Li, D., and Sun, Z. (2020). Anticoagulant treatment is associated with  
23 decreased mortality in severe coronavirus disease 2019 patients with coagulopathy. *J. Thromb. Haemost.*  
24 *18*, 1094–1099.
- 25 Tetro J. A. (2020). Is COVID-19 receiving ADE from other coronaviruses? *Microb. Infect.* *22*, 72–73.
- 26 Thompson, B.T., Chambers, R.C., and Liu, K.D. (2017). Acute respiratory distress syndrome. *N. Engl. J. Med.*  
27 *377*, 562–572.
- 28 Tricou, V., Minh, N. N., Van, T. P., Lee, S. J., Farrar, J., Wills, B., Tran, H. T., and Simmons, C. P. (2010). A  
29 randomized controlled trial of chloroquine for the treatment of dengue in Vietnamese adults. *PLoS Negl.*  
30 *Trop. Dis.* *4*, e785.
- 31 Vankadari, N., and Wilce, J. A. (2020). Emerging WuHan (COVID-19) coronavirus: glycan shield and  
32 structure prediction of spike glycoprotein and its interaction with human CD26. *Emerg. Microbes Infect.* *9*,  
33 601–604.
- 34 Walls, A. C., Xiong, X., Park, Y. J., Tortorici, M. A., Snijder, J., Quispe, J., Cameroni, E., Gopal, R., Dai, M.,  
35 Lanzavecchia, A., et al. (2019). Unexpected receptor functional mimicry elucidates activation of  
36 coronavirus fusion. *Cell* *176*, 1026–1039.
- 37 Walls, A. C., Park, Y. J., Tortorici, M. A., Wall, A., McGuire, A. T., and Velesler, D. (2020). Structure, function,  
38 and antigenicity of the SARS-CoV-2 spike glycoprotein. *Cell* *181*, 281–292.
- 39 Wan, Y., Shang, J., Sun, S., Tai, W., Chen, J., Geng, Q., He, L., Chen, Y., Wu, J., Shi, Z., et al. (2020). Molecular  
40 mechanism for antibody-dependent enhancement of coronavirus entry. *J. Virol.* *94*, e02015-19.
- 41 Wang, H., Yang, P., Liu, K., Guo, F., Zhang, Y., Zhang, G., and Jiang, C. (2008). SARS coronavirus entry into  
42 host cells through a novel clathrin- and caveolae-independent endocytic pathway. *Cell Res.* *18*, 290–301.
- 43 Wang, M., Cao, R., Zhang, L., Yang, X., Liu, J., Xu, M., Shi, Z., Hu, Z., Zhong, W., and Xiao, G. (2020).  
44 Remdesivir and chloroquine effectively inhibit the recently emerged novel coronavirus (2019-nCoV) in

- 1 vitro. *Cell Res.* 30, 269–271.
- 2 Watanabe, R., Sawicki, S. G., and Taguchi, F. (2007). Heparan sulfate is a binding molecule but not a  
3 receptor for CEACAM1-independent infection of murine coronavirus. *Virology* 366, 16–22.
- 4 Waterhouse, A., Bertoni, M., Bienert, S., Studer, G., Tauriello, G., Gumienny, R., Heer, F. T., de Beer, T. A. P.,  
5 Rempfer, C., Bordoli, L., et al. (2018). SWISS-MODEL: homology modelling of protein structures and  
6 complexes. *Nucleic Acids Res.* 46, W296–W303.
- 7 Xia, S., Liu, M., Wang, C., Xu, W., Lan, Q., Feng, S., Qi, F., Bao, L., Du, L., Liu, S., et al. (2020). Inhibition of  
8 SARS-CoV-2 (previously 2019-nCoV) infection by a highly potent pan-coronavirus fusion inhibitor targeting  
9 its spike protein that harbors a high capacity to mediate membrane fusion. *Cell Res.* 30, 343–355.
- 10 Xu, K., Chen, Y., Yuan, J., Yi, P., Ding, C., Wu, W., Li, Y., Ni, Q., Zou, R., Li, X., et al. (2020). Factors associated  
11 with prolonged viral RNA shedding in patients with COVID-19. *Clin. Infect. Dis.* DOI: 10.1093/cid/ciaa351.
- 12 Yamamoto, M., Matsuyama, S., Li, X., Takeda, M., Kawaguchi, Y., Inoue, J.I., and Matsuda, Z. (2016).  
13 Identification of nafamostat as a potent inhibitor of middle east respiratory syndrome coronavirus S  
14 protein-mediated membrane fusion using the split-protein-based cell-cell fusion assay. *Antimicrob. Agents*  
15 *Chemother.* 60, 6532–6539.
- 16 Yan, R., Zhang, Y., Li, Y., Xia, L., Guo, Y., and Zhou, Q. (2020). Structural basis for the recognition of  
17 SARS-CoV-2 by full-length human ACE2. *Science* 367, 1444–1448.
- 18 Yao, X., Ye, F., Zhang, M., Cui, C., Huang, B., Niu, P., Liu, X., Zhao, L., Dong, E., Song, C., et al. (2020). In vitro  
19 antiviral activity and projection of optimized dosing design of hydroxychloroquine for the treatment of  
20 severe acute respiratory syndrome coronavirus 2 (SARS-CoV-2). *Clin. Infect. Dis.* DOI: 10.1093/cid/ciaa237.
- 21 Yin, S., Huang, M., Li, D., and Tang, N. (2020). Difference of coagulation features between severe  
22 pneumonia induced by SARS-CoV2 and non-SARS-CoV2. *J. Thromb. Thrombolysis* DOI:  
23 10.1007/s11239-020-02105-8.
- 24 Yu, J., Tostanoski, L. H., Peter, L., Mercado, N. B., McMahan, K., Mahrokhian, S. H., Nkolola, J. P., Liu, J., Li, Z.,  
25 Chandrashekar, A., et al. (2020). DNA vaccine protection against SARS-CoV-2 in rhesus macaques. *Science*  
26 DOI: 10.1126/science.abc6284.
- 27 Yuan, S., Jiang, S. C., and Li, Z. L. (2020a). Analysis on possible intermediate hosts of the new coronavirus  
28 SARS-CoV-2. *Front. Vet. Sci.* 7, 379.
- 29 Yuan, S., Jiang, S. C., and Li, Z. L. (2020b). Early oxygen inhalation to prevent SARS-CoV-2-induced acute  
30 respiratory distress syndrome. Preprints DOI: 10.20944/preprints202004.0360.v1.
- 31 Zhang, B., Zhou, X., Zhu, C., Feng, F., Qiu, Y., Feng, J., Jia, Q., Song, Q., Zhu, B., and Wang, J. (2020). Immune  
32 phenotyping based on neutrophil-to-lymphocyte ratio and IgG predicts disease severity and outcome for  
33 patients with COVID-19. medRxiv DOI: 10.1101/2020.03.12.20035048.
- 34 Zhao, J., Yuan, Q., Wang, H., Liu, W., Liao, X., Su, Y., Wang, X., Yuan, J., Li, T., Li, J., et al. (2020). Antibody  
35 responses to SARS-CoV-2 in patients of novel coronavirus disease 2019. *Clin. Infect. Dis.* DOI:  
36 10.1093/cid/ciaa344.
- 37 Zheng, M., and Song, L. (2020). Novel antibody epitopes dominate the antigenicity of spike glycoprotein in  
38 SARS-CoV-2 compared to SARS-CoV. *Cell. Mol. Immunol.* 17, 536–538.
- 39 Zhu, F. C., Li, Y. H., Guan, X. H., Hou, L. H., Wang, W. J., Li, J. X., Wu, S. P., Wang, B. S., Wang, Z., Wang, L., et  
40 al. (2020). Safety, tolerability, and immunogenicity of a recombinant adenovirus type-5 vectored COVID-19  
41 vaccine: a dose-escalation, open-label, non-randomised, first-in-human trial. *Lancet* DOI:  
42 10.1016/S0140-6736(20)31208-3.
- 43 Zumla, A., Hui, D. S., Azhar, E. I., Memish, Z. A., and Maeurer, M. (2020). Reducing mortality from  
44 2019-nCoV: host-directed therapies should be an option. *Lancet* 395, e35–e36.
- 45

1  
2  
3  
4  
5  
6  
7  
8  
9  
10  
11  
12  
13  
14  
15  
16  
17  
18  
19  
20  
21  
22  
23  
24  
25  
26  
27  
28  
29  
30  
31  
32  
33  
34  
35  
36  
37  
38  
39  
40  
41  
42  
43  
44

## LEAD CONTACT AND MATERIALS AVAILABILITY

Requests for material can be directed to Shu Yuan ([roundtree318@hotmail.com](mailto:roundtree318@hotmail.com)). All materials and reagents will be made available upon installment of a material transfer agreement (MTA).

## METHOD DETAILS

### Homology modeling of ACE2 and viral spike proteins

All full-length protein sequences were downloaded from National Center of Biotechnology Information (NCBI; <https://www.ncbi.nlm.nih.gov/>). The sequence of human angiotensin-converting enzyme 2 (ACE2, Accession ID: BAB40370.1), SARS-CoV CUHK-W1 Spike (S) protein (AAP13567.1) and SARS-CoV-2 WHU01 S protein (QHO62107.1) were subjected to the analysis of homology models which were constructed in the SWISS-MODEL Workspace (Bertoni et al., 2017; Biasini et al. 2014; Bienert et al. 2017; Waterhouse et al. 2018; <http://swissmodel.expasy.org/workspace/>). The optimal templates for ACE2 was 6m17.1.B with a sequence identity of 99.87% and a coverage from 21-768 aa (805 aa totally). The optimal templates for SARS-CoV S was 6acd.1.A with a sequence identity of 99.83% and a coverage from 18-1119 aa (1255 aa totally). The optimal templates for SARS-CoV-2 S was 6vsb.1.A with a sequence identity of 99.26% and a coverage from 27-1146 aa (1273 aa totally).

The Molecular surface and the electrostatic potential were computed with the Swiss-PdbViewer v4.1.0 software (Bertoni et al., 2017; Biasini et al. 2014; Bienert et al. 2017; Waterhouse et al. 2018). To see every amino acid no matter covered or uncovered by the protein surface, transparency of the surface was set at 30%.

### Analysis of antibody epitopes and glycosylation sequons

SARS-CoV CUHK-W1 Spike (S) protein (AAP13567.1) and SARS-CoV-2 WHU01 S protein (QHO62107.1) were subjected to the analysis of antibody epitopes. The sequence-based antibody epitopes score was predicted according to the epitope surface accessibility (SA) by using Emini surface accessibility scale method (Emini et al., 1985; <http://tools.iedb.org/bcell/>). The possible antibody epitopes were filtered by the surface accessible scores using the default threshold value of 1.0 with a center position of 3 aa and a window size of 6 aa. Then the epitope candidates were re-scored by using BepiPred-2.0 bioinformatic tool with the default threshold value of 0.50 (Jespersen et al., 2017; <http://tools.iedb.org/bcell/>). The average score of each epitope was calculated based on the epitope score of each amino acid. Epitopes with average scores below 0.5 were ruled out. 27 epitopes were found on SARS-CoV S protein, among which 10 epitopes had been ruled out due to the low epitope scores. 30 epitopes were found on SARS-CoV-2 S protein, among which 9 epitopes had been ruled out due to the low epitope scores. Finally, 17 predicted epitopes for the SARS-CoV S protein and 21 predicted epitopes for the SARS-CoV-2 S protein were screened out and are shown in Tables S1 and S2.

N-linked glycosylation sites in SARS-CoV S and SARS-CoV-2 S are marked on the protein surface based on the sequons identified by Walls et al. (2020).

### Prediction of transmembrane domain

Human transmembrane serine protease 2 (TM PRSS2) precursor zymogen (AF123453.1) and cleaved active enzyme (AAK29280.1), human ACE2 (BAB40370.1), SARS-CoV CUHK-W1 S protein (AAP13567.1) and SARS-CoV-2 WHU01 S protein (QHO62107.1) were subject to the transmembrane domain analysis. The putative transmembrane helices were scored by using TMHMM Server v. 2.0 bioinformatic tool (Krogh et



1 al., 2001; Moller et al., 2001; <http://www.cbs.dtu.dk/services/TMHMM/>).

2

### 3 **Alignment of SARS-CoV and SARS-CoV-2 spike proteins**

4 In a phylogenetic network analysis of SARS-CoV-2 genomes, three central variants distinguished by amino  
5 acid changes were defined, which we have named A, B, and C types (Forster et al., 2020). Three  
6 representative Sprotein sequences of SARS-CoV-2 USA-WA1/2020 (QHO60594.1) for the type A virus strain,  
7 SARS-CoV-2 WHU01 (QHO62107.1) for the type B virus strain and SARS-CoV-2 SNU01 (QHZ00379.1) for the  
8 type C virus strain were collected. Along with the SARS-CoV CUHK-W1 S protein sequence (AAP13567.1),  
9 these four amino acid sequences were aligned using the software ClustalX2.1 (Larkin et al., 2007).

10

### 11 **QUANTIFICATION AND STATISTICAL ANALYSIS**

12 Clinical data of cancer patients with confirmed SARS-CoV-2 infections (Montopoli et al., 2020) were  
13 re-analyzed. One-way analysis of variance (ANOVA) was used to test for statistical significance. Only p  
14 values of 0.05 or lower were considered statistically significant. For all statistical analyses, the SPSS 22.0  
15 software package was used.

16

### 17 **DATA AND CODE AVAILABILITY**

18 The study did not generate unique datasets or code.